Dichotomy in the Reactivity of Trivalent Phosphorus Compounds Z_3P (Z = Ph, *n*Bu, OR) Observed in the Photoreaction with a Ruthenium Complex

Shinro Yasui*[a], Munekazu Tsujimoto[a], Kosei Shioji[b], and Atsuyoshi Ohno[b]

Laboratory of Biology and Chemistry, Tezukayama College[a],
Gakuen-Minami, Nara 631, Japan

Institute for Chemical Research, Kyoto University[b],
Uji, Kyoto 611, Japan

Received April 17, 1997

Keywords: Trivalent phosphorus / Ruthenium / Photolysis / Electron transfer / Ligand exchange

Solutions of tris(2,2'-bipyridyl)ruthenium(II) dichloride ($\mathbf{Ru^{2+}}$) and various types of trivalent phosphorus compounds Z_3P (Z = Ph, *n*Bu, OR; **1**) in methanol have been photolyzed with visible light at 20 °C under an argon atmosphere, resulting in the oxidation of **1** to the corresponding pentavalent oxo compounds $Z_3P{=}O$ and ligand exchange of $\mathbf{Ru^{2+}}$ with **1**. The former process takes place via single-electron transfer (SET) from **1** to $\mathbf{Ru^{2+}}$ in the photoexcited state, $\mathbf{Ru^{2+}}$*, which generates the radical cation intermediate $Z_3P^{\bullet+}$ from **1**. The latter results from nucleophilic attack of **1** upon $\mathbf{Ru^{2+}}$*. The results show that **1** can act either as an electron donor or as a nucleophile toward $\mathbf{Ru^{2+}}$*. The rate constants for both processes are estimated. An excellent linear correlation is found between the logarithm of the SET rate and the oxidation potential for both the aromatic and aliphatic trivalent phosphorus compounds examined here; the slope of the plot is much less negative than expected on the basis of Rehm-Weller theory. Such behavior in the SET rates is interpreted by comparison with SET quenching by amines. On the other hand, a dual-parameter correlation analysis shows that the ligand exchange is regulated by both steric and electronic factors in **1**.

Trivalent phosphorus compounds Z_3P undergo nucleophilic attack on an electrophilic center in a highly exothermic process to produce rather stable phosphonium ions (Process A in Scheme 1).

Scheme 1. Possible reaction pathways of Z_3P

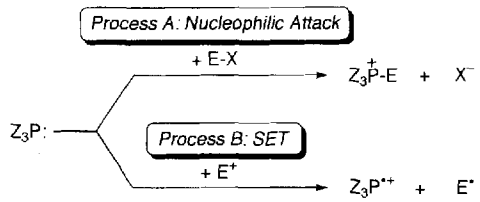

Based on such reactivity of Z_3P, several "name" reactions, e.g. the Wittig, the Arbuzov, and the Mitsunobu reactions, have been developed[1]. Meanwhile, it has become well known that these phosphorus compounds can also act as one-electron donors with good electron acceptors. Thus, ourselves[2][3][4][5] and others[6][7][8][9] have found single electron transfer (SET) occurring from Z_3P to electron-deficient compounds such as acridinium salts in the photoexcited state[3], diazonium salts[4], and methylviologen[5], thereby generating the corresponding radical cations $Z_3P^{\bullet+}$ (Process B in Scheme 1).

Ruthenium(II) complexes are good electron acceptors when photoexcited[10][11][12][13][14]. In addition, when ligated by bipyridyl (bpy) ligands, such complexes undergo ligand exchange with nucleophiles under the photochemical conditions[15][16][17][18][19]. In this context, it is of particular interest too ascertain what type of reaction takes place when a Ru^{II} complex having bpy ligands is photolyzed in the presence of Z_3P; does Z_3P donate an electron to the ruthenium complex? Does it attack the complex in a nucleophilic fashion to bring about ligand exchange?

We have examined the photoreaction of tris(2,2'-bipyridyl)ruthenium(II) dichloride, $[Ru^{II}(bpy)_3]^{2+} \cdot 2\ Cl^-$ ($\mathbf{Ru^{2+}}$), with various types of trivalent phosphorus compounds Z_3P (**1a–j**) and have found that **1** quenches the photoexcited state of $\mathbf{Ru^{2+}}$, $\mathbf{Ru^{2+}}$*, through SET, while ligand exchange reaction of $\mathbf{Ru^{2+}}$* with **1** takes place competitively. This is the first observation of Z_3P simultaneously acting as a one-electron donor *and* as a nucleophile toward a single reagent under a specific set of conditions. The photoreaction is a useful tool, not only for individually investigating the energetics of the SET from **1** to $\mathbf{Ru^{2+}}$* and the ligand exchange of $\mathbf{Ru^{2+}}$* with **1**, but also to find factors which determine the relative importance of one-electron donor character and nucleophilic character in a given trivalent phosphorus compound.

In this paper, we report on kinetic analysis of the photoreaction of **1** with $\mathbf{Ru^{2+}}$ and, based on the rate constants obtained, we discuss the energetics of the two distinct processes occurring in the photoreaction. After that, we present our assessment of how the one-electron donor character and the nucleophilic character of **1** are related to each other. Of special importance here is the determination of rate constants for the SET from **1**; there has hitherto been no report

  0009–2940/97/1111–1699 $ 17.50+.50/0

on the kinetics of SET from trivalent phosphorus compounds.

Results

Spectrophotometry: Solutions of $\mathbf{Ru}^{2+}$ in methanol ($2.50 \cdot 10^{-5}$ M) were photolyzed with light from a xenon lamp ($\lambda > 360$ nm with a sharp-cut glass filter) in the presence of a large excess of **1** ($2.50 \cdot 10^{-4}$ M) under an argon atmosphere at 20 °C. Spectrophotometric analysis showed that $\mathbf{Ru}^{2+}$ was consumed gradually with simultaneous increase in an absorption at around 500 nm, which is characteristic of the one-electron reduced form of $\mathbf{Ru}^{2+}$, $Ru^{I}(bpy)_3^+$ ($\mathbf{Ru}^{+}$)[12][13]. The absorption change exhibited no clear isosbestic points. Examples are presented in Figures 1a and 1b for the reactions with triphenylphosphane (**1b**) and trimethyl phosphite (**1h**), respectively.

Figure 1. UV/visible spectral change accompanying the photoreaction of $\mathbf{Ru}^{2+}$ in the presence of a large excess of **1** in methanol. (a) With **1b**; recorded at 0, 15, 30, 60, 90, 120, 180, 240, 300, 360, and 480 minutes. – (b) With **1h**; recorded at 0, 15, 30, 45, 60, 90, 120, 180, 240, 300, 360, and 480 minutes.

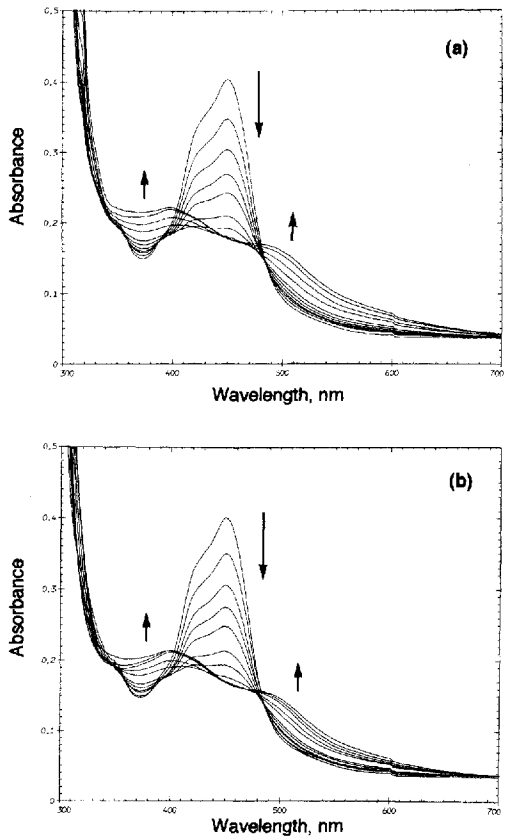

The absorption from $\mathbf{Ru}^{2+}$ decreased even in the absence of **1**, albeit more slowly, the reaction mixture eventually giving a UV/visible spectrum similar to that obtained in the presence of **1** (Figure 2).

In this case, a clear isosbestic point was observed at 481 nm. Without irradiation, $\mathbf{Ru}^{2+}$ was stable in methanol both in the presence and in the absence of **1**.

Product Analysis: The photoreaction of equimolar amounts of **1a–j** and $\mathbf{Ru}^{2+}$ ($5.00 \cdot 10^{-3}$ M) was carried out in methanol under the conditions described above. After ca. 4–5 h, the reaction mixture was analyzed by GC and GCMS, which showed the formation of the corresponding oxidation product **2a–j** from **1a–j**, along with 2,2′-bipyridine (bpy). No other product could be detected by GC. The yields of the products as well as the percent conversions of **1** are summarized in Table 1.

Figure 2. UV/visible spectral change accompanying the photoreaction of $\mathbf{Ru}^{2+}$ in methanol in the absence of **1**. Recorded at 0, 15, 30, 45, 60, 90, 120, 180, 240, 300, 360, and 480 minutes.

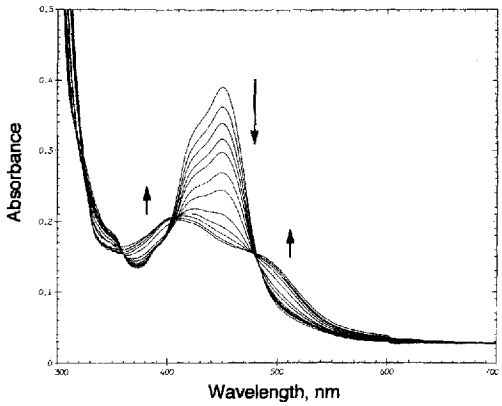

Table 1. Photoreaction of trivalent phosphorus compound **1** with $[Ru(bpy)_3]^{2+}$ ($\mathbf{Ru}^{2+}$)[a,b]

entry	1	Time [h]	Conv. of **1** [%][c,d]	2	Yield [%][c] **Ru-P**[e]	bpy[f]
1	**1a**	5	14.6	13.3	1.3	0
2	**1b**	5	25.7	13.5	12.2 (11)[g]	0
3	**1c**	5	75.5	14.0[h]	61.5	0
4	**1d**	5	44.5	12.1	32.4	13.9
6	**1e**	5	47.1	30.1[i]	17.0 (14)[g]	18.2
7	**1f**	5	56.0	6.3	49.7	7.5
8	**1g**	5	84.2	14.0[i]	70.2	11.7
9	**1h**	7	51.5	4.7	46.8	6.1
10	**1i**	7	59.8	8.7[i]	51.1	10.1
11	**1j**	7	57.6	10.3[i]	47.3	8.8

[a] Xenon lamp; $\lambda > 360$ nm with a sharp-cut glass filter. – [b] In methanol at 20 °C under an argon atmosphere. $[\mathbf{1}]_0 = [\mathbf{Ru}^{2+}]_0 = 5.00 \cdot 10^{-3}$ M. – [c] Based on $[\mathbf{1}]_0$; determined by GC. – [d] Percent conversion of **1**. – [e] Assuming that yield(**Ru-P**) =%conv.(**1**) – yield(**2**). – [f] Yield of 2,2′-bipyridine. – [g] Isolated yield. – [h] In the absence of $\mathbf{Ru}^{2+}$, **1c** was oxidized to afford 5.8% of **2c** after photolysis for this length of time. – [i] Total yield of the ethyl (or isopropyl) ester and the esters in which one or more ethyl (or isopropyl) groups have been replaced by methyl group(s) from the solvent methanol.

No decomposition of **1** was observed in the absence of $\mathbf{Ru}^{2+}$ either under irradiation or in the dark, except in the case of **1c**; photooxidation of **1c** took place in the absence of $\mathbf{Ru}^{2+}$ to give 5.8% of **2c** after 5 h of photolysis.

Non-volatile products were isolated from the photoreaction of $\mathbf{Ru}^{2+}$ with **1b** or **1e**. One of these products was identified as $[Ru^{II}(bpy)_2(PZ_3)Cl]^+$ [PZ_3 = PPh_3 (**Ru-P-b**) or PZ_3 = $PPh_2(OEt)$ (**Ru-P-e**)] based on comparison of its UV/visible and NMR spectra with those of an authentic sample. The absorption pattern, which exhibited absorption maxima at 330 nm and 465 nm, was similar to those reported for $[Ru^{II}(bpy)_2(py)X]^+$ (X = NO_2^-, NO_3^-, and ClO_4^-)[17]. The isolated yields of **Ru-P-b** and **Ru-P-e** were

determined on the basis of the absorbance at 465 nm (Table 1). When a larger amount of **1b** was used, **Ru-P-b** was obtained in a higher yield. Two phosphorus-free ruthenium complexes were also found in lower yields in each reaction. By comparison of their spectra with those of authentic samples, these were identified as the starting material $\mathbf{Ru}^{2+}$ and $[Ru^{II}(bpy)_2Cl_2]$ (**Ru-Cl**) (λ_{max} = 380 and 556 nm)[17]. Clearly, these complexes result from oxidation of $\mathbf{Ru}^{+}$ during the work-up procedure and further replacement of the ligand in **Ru-P** by Cl^-, respectively.

The photolysis of $\mathbf{Ru}^{+}$ with **1b** or **1d** in methanol was also carried out using monochromatic light at 450 nm under otherwise identical conditions. After 5 h, the percent conversion of **1** and the yield of **2** were determined by GC (Table 2).

Table 2. Photoreaction of **1** with $\mathbf{Ru}^{2+}$ under the irradiation of monochromatic light at 450 nm[a,b]

entry	**1**	Conv. of **1** [%][c,d]	**2**	Yield [%][c] **Ru-P**[e]
1	**1b**	39.6 (0.016)	19.7 (0.0078)	19.9 (0.0078)
2	**1d**	43.2 (0.017)	10.2 (0.0040)	33.0 (0.013)

[a] Xenon lamp with an interference filter. Reaction time; 5 h. Numbers in parentheses denote quantum yields. – [b–e] See footnotes [b–e] in Table 1, respectively.

The intensity of the incident light at 450 nm under our experimental conditions was determined using a potassium ferrioxalato actinometer to be $1.76 \cdot 10^{-6}$ einstein $\cdot s^{-1} cm^{-2}$. This value was used to calculate the quantum yields of the products, which are listed in Table 2.

The results of spectrophotometric and product analyses showed that the present photoreaction between **1** and $\mathbf{Ru}^{2+}$ affords **2**, $\mathbf{Ru}^{+}$ and **Ru-P**, along with bpy (eq. 1).

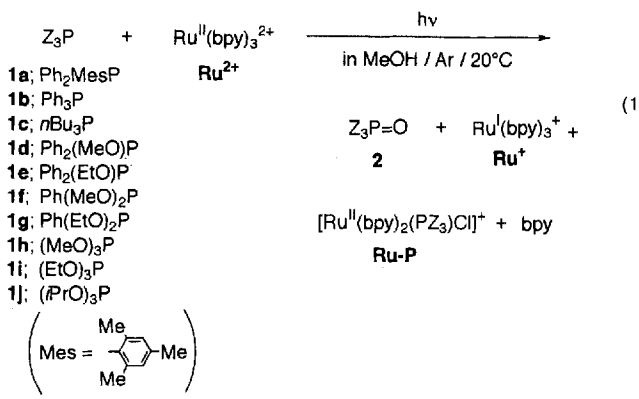

(1)

Kinetics: Kinetic measurements were made on the photoreaction under pseudo-first-order conditions with **1** being present in large excess, and the disappearance of $\mathbf{Ru}^{2+}$ was followed by periodically monitoring the luminescence from $\mathbf{Ru}^{2+}$* on a spectrofluorophotometer. Linear dependence of $[\mathbf{Ru}^{2+}]$ on the intensity of the luminescence over the range of concentrations used here was confirmed independently. Logarithmic plots of $[\mathbf{Ru}^{2+}]$ vs. time gave straight lines for a range of more than three half-lives (correlation coefficient $r > 0.9990$), and from the slopes of these observed pseudo-first-order rate constants k^{obs} were determined[20]. Experiments were performed at different concentrations of **1**, and k^{obs} was plotted against $[\mathbf{1}]_0$. Each of the straight line plots obtained for the compounds **1a–j** gave a common value for the intercept, which approximated to the first-order rate constant for photodecomposition of $\mathbf{Ru}^{2+}$, k_d^{obs} (= $2.16 \cdot 10^{-4}$ s^{-1}), determined in the absence of **1** (Figure 3).

Figure 3. Plot of k^{obs} vs. $[\mathbf{1}]_0$

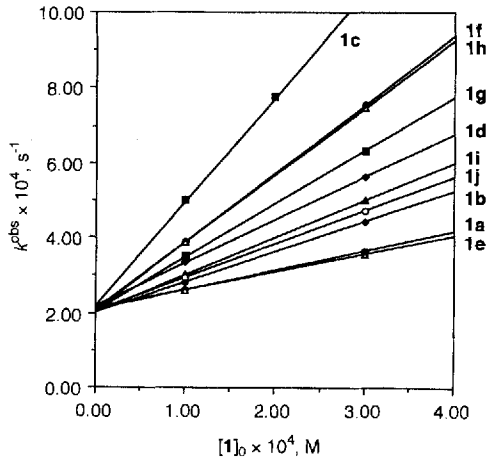

The findings show that decrease in $[\mathbf{Ru}^{2+}]$ follows second-order kinetics represented by eq. 2, with the second-order rate constant k_{exp}. The values of k_{exp}, each of which was determined from the slope of the plots in Figure 3, are summarized in Table 3.

Table 3. Kinetic parameters for the photoreaction of **1** with $\mathbf{Ru}^{2+}$[a]

entry	**1**	$k_{exp} \cdot 10$[a] [$M^{-1}s^{-1}$]	$ak_c \cdot 10$[b] [$M^{-1}s^{-1}$]	$ak_x \cdot 10$[b] [$M^{-1}s^{-1}$]
1	**1a**	5.15	2.35	0.459
2	**1b**	7.95	2.09	3.77
3[c]	**1b**	0.570	0.142	0.286
4	**1c**	27.8	1.64[d]	24.5[d]
5	**1d**	11.6	1.58	8.44
6[c]	**1d**	0.850	0.101	0.0649
7	**1e**	4.75	1.52	1.71
8	**1f**	18.3	1.03	16.2
9	**1g**	14.2	1.18	11.8
10	**1h**	18.0	0.821	16.4
11	**1i**	9.95	0.724	8.50
12	**1j**	8.90	0.796	7.31

[a] Xenon lamp; $\lambda > 360$ nm unless otherwise noted. In methanol at 20 °C under an argon atmosphere. $[\mathbf{1}]_0 = (1.0–3.0) \cdot 10^{-4}$ M. $[\mathbf{Ru}^{2+}]_0 = 1.0 \cdot 10^{-5}$ M. – [b] Evaluated based on $k_{exp} = a(2k_c + k_x)$; see the text. – [d] Calculated taking into account that **1c** is oxidized (5.8%) in the absence of $\mathbf{Ru}^{2+}$ under these conditions. – [c] Irradiated with monochromatic light at 450 nm.

$$-d[\mathbf{Ru}^{2+}]/dt = (k_{exp}[\mathbf{1}] + k_d^{obs})[\mathbf{Ru}^{2+}] \quad (2)$$

Kinetic studies of the reactions with **1b** and **1d** were also carried out by irradiation with monochromatic light at 450 nm under otherwise identical conditions. The decrease in $[\mathbf{Ru}^{2+}]$ again followed eq. 2 with the second-order rate constant k_{exp} (entries 3 and 6 in Table 3)[21].

Discussion

Mechanism: Under our photochemical conditions, Ru^{2+} is photoexcited to its metal-to-ligand charge-transfer (MLCT) photoexcited state, $Ru^{2+}*$, which is known to be a good oxidant (eq. 3)[10][11].

$$Ru^{2+} \xrightarrow{h\nu} Ru^{2+*} \qquad (3)$$

Meanwhile, the ability of trivalent phosphorus compounds to act as one-electron donors has been well documented[2][3][4][5][6][7][8][9][22]. Therefore, $Ru^{2+}*$ is quenched by single-electron transfer (SET) from **1**, generating Ru^{+} as well as the radical cation $\mathbf{1}^{\bullet+}$ (eq. 4, path a).

$$\mathbf{1} + Ru^{2+*} \begin{cases} \xrightarrow[\text{path a}]{k_e} Z_3P^{\bullet+} + Ru^{+} \quad (\mathbf{1}^{\bullet+}) \\ \xrightarrow[\text{path b}]{k_x} \text{Ru-P} \end{cases} \qquad (4)$$

The formation of the oxidation product **2** is evidence for generation of $\mathbf{1}^{\bullet+}$. As has been observed previously[3][4][5], $\mathbf{1}^{\bullet+}$ reacts with methanol to give a phosphoranyl radical $\mathbf{3}^{\bullet}$, which collapses to **2** through another SET to $Ru^{2+}*$. This is followed by elimination of a methyl cation equivalent from the resulting phosphonium ion $\mathbf{3}^{+}$ (eq. 5).

$$\mathbf{1}^{\bullet+} + \text{MeOH} \xrightarrow[-H^+]{k_m} \underset{\mathbf{3}^{\bullet}}{Z_3\dot{P}\text{-OMe}} \xrightarrow[fast]{Ru^{2+*}\ Ru^{+}\ \text{SET}} \underset{\mathbf{3}^{+}}{Z_3\overset{+}{P}\text{-OMe}} \xrightarrow{-Me^+} \mathbf{2} \qquad (5)$$

The SET from $\mathbf{3}^{\bullet}$ to $Ru^{2+}*$ in this reaction sequence is highly exothermic and takes place in a practically irreversible way, since peak potentials of **1a–j**, E_p^{ox}, which were determined by cyclic voltammetry in acetonitrile as listed in Table 4, are significantly higher than the reported values for half-wave potentials of phosphonium cations [$E_{1/2}$ = −2.15 – (−1.66) V vs. SCE][23]. β-Scission of **3•**, which could afford **2** directly, is not likely to occur because the process would produce a very unstable methyl radical[3][5][24]. In addition, the reactions of the ethyl esters **1e**, **1g**, and **1i**, and of the isopropyl ester **1j**, give products that result from transesterification with the solvent. Among these products, the esters in which more than one ethyl (or isopropyl) groups are replaced by methyl groups from the solvent are formed only via the phosphonium cation intermediate $\mathbf{3}^{+}$[4d].

The photoreaction of Ru^{2+} with **1** also produces the ruthenium complex **Ru-P**, which contains **1** as a ligand, thereby demonstrating that ligand exchange of $Ru^{2+}*$ with **1** takes place under the photochemical conditions (eq. 4, path b), in competition with the SET process (eq. 4, path a). It is known that the bpy ligand in Ru^{2+} or related complexes is easily replaced by amines or anions such as Cl^-, NCS^-, or NO_3^- under photochemical conditions[15][16][17][18][19]. The isolated yields of **Ru-P-b** (11%) and **Ru-P-e** (14%) from the reactions with **1b** and **1e**, respectively, account well for the discrepancy found between the percent conversion of **1** and the yield of **2** (25.7% − 13.5% = 12.2% for **1b** and 47.1% − 30.1% = 17.0% for **1e**, respectively) (entries 2 and 6 in Table 1). Thus, in Table 1 the discrepancies are listed as the yield of **Ru-P** for each reaction.

Table 4. Pertinent parameters of **1**

1	E_p^{ox}[a] [V]	θ [b] [deg.]	ν[c] [cm^{-1}]
1a	0.82	167	2067.4
1b	0.94	145	2068.9
1c	1.10	132	2060.3
1d	1.24	132	2072.0
1e	1.20	133	2071.6
1f	1.52	115	2075.8
1g	1.50	116	2074.6
1h	1.84	107	2079.5
1i	1.90	109	2076.3
1j	1.86	130	2075.9

[a] Peak potential vs. Ag/Ag^+. Determined in acetonitrile using Et_4NBF_4 (0.10 M) as the supporting electrolyte. – [b] Cone angle. Data from ref.[34b] – [c] CO stretching frequency ν of $Ni(CO)_3(Z_3P)$. Data from refs.[34a][35].

The change in the UV/visible spectrum during the course of photolysis does not exhibit clear isosbestic points (Figure 1), suggesting that Ru^{2+} is consumed via a multistep mechanism. In fact, photochemical ligand exchange of Ru^{2+} with amines, NCS^-, or OH^- has also been found to proceed without showing clear isosbestic points in the accompanying spectral change[17][19]. This observation has led to the conclusion that the bpy ligand in Ru^{2+} is replaced by nucleophiles in a stepwise fashion via a monodentate intermediate that bears a singly bound bpy ligand. Our observation in Figure 1 can therefore be attributed to a stepwise ligand exchange occurring via a monodentate complex, $[Ru^{II}(bpy)_2PZ_3(bpy)]^+$ (**Ru-P'**). In contrast, photolysis of a solution of Ru^{2+} in the absence of **1**, in the course of which Ru^{2+} is consumed solely through the photochemical reduction to Ru^+, results in a similar spectral change, but an isosbestic point at 481 nm is distinct throughout the photolysis (Figure 2).

The ligand exchange should liberate a bpy ligand, which indeed was detected by GC. However, in most cases the yield of bpy was lower than expected. Since it is a more polar molecule than **1** or **2**, some bpy was probably lost during the treatment of the reaction mixture on silica gel prior to GC injection (see Experimental Section). Another possibility, although it seems less likely, is that in some cases a monodentate complex **Ru-P'** initially formed during the photoreaction is reluctant to collapse to **Ru-P** and bpy (eq. 6)[17][19], thereby lowering the yield of bpy detected by GC.

$$\mathbf{1} + Ru^{2+*} \xrightarrow{k_x} \underset{\text{Ru-P'}}{[Ru^{II}(bpy)_2(PZ_3)(bpy)]^{2+}} \xrightarrow[-\text{bpy}]{} \text{Ru-P} \qquad (6)$$

In other words, although not sufficiently stable to be isolated, **Ru-P'** is a product of ligand exchange in the reaction mixture[19]. If such a mechanism were operative here, the observation that bpy is detected only in the photoreactions with trivalent phosphorus compounds containing a P–O bond (see Table 1) gives an indication of the stability of phosphorus-to-metal coordination in organometallic com-

plexes. At present, however, we do not have further data to allow more detailed discussion of this point.

In conclusion, the photoreaction of **1** with Ru^{2+} results in both SET from **1** to $Ru^{2+}*$ and in ligand exchange of $Ru^{2+}*$ with **1**. For a complete mechanistic picture of the present photoreaction, several side reactions also need to be considered. Gradual disappearance of Ru^{2+} observed even in the absence of **1** in methanol (Figure 2) may result from SET quenching of $Ru^{2+}*$ by the solvent[25]; this process would be favored by being coupled with energy-gaining decomposition of the resulting methanol cation radical to formaldehyde (eq. 7). Meanwhile, Ru^{2+} is regenerated through decay of $Ru^{2+}*$ (eq. 8) and "back" electron-transfer from Ru^{+} to $1^{\bullet+}$ in the ground state (eq. 9). Thus, the present photoreaction consists of the individual reactions summarized in Scheme 2.

$$Ru^{2+*} + MeOH \xrightarrow[SET]{k_d} Ru^{+} + (MeOH)^{\bullet+} \xrightarrow{-H^+} {}^{\bullet}CH_2OH \longrightarrow CH_2{=}O \quad (7)$$

$$Ru^{2+*} \xrightarrow{k_o} Ru^{2+} \quad (8)$$

$$1^{\bullet+} + Ru^{+} \xrightarrow{k_b} 1 + Ru^{2+} \quad (9)$$

Kinetic Analysis of the Photoreaction: According to Scheme 2, the disappearance of Ru^{2+} is expressed by

$$-d[Ru^{2+}]/dt = \phi' I_a - k_o[Ru^{2+}*] - k_b[1^{\bullet+}][Ru^{+}] \quad (10)$$

where ϕ' and I_a are the efficiency of populating $Ru^{2+}*$[27] and the intensity of the light absorbed by Ru^{2+}, respectively.

The rate constant for the ionic reaction of $1c^{\bullet+}$ with methanol, k_m, has been estimated to be of the order of 10^6 $M^{-1}s^{-1}$[5][28]. Meanwhile, [MeOH] = 25 M and the maxima of k_b and $[Ru^{+}]$ are 10^{10} $M^{-1}s^{-1}$ and 10^{-5} M, respectively, under our experimental conditions. Thus, $k_b[Ru^{+}] << k_m[MeOH]$. Using this approximation and assuming steady-state concentrations of $Ru^{2+}*$, $1^{\bullet+}$, and $3^{\bullet}$, eq. (10) can ultimately be expressed as eq. (11).

$$-d[Ru^{2+}]/dt = \frac{\phi' I_a\{(2k_e + k_x)[1] + k_d\}}{(2k_e + k_x)[1] + k_d + k_o} \quad (11)$$

It has been shown that ϕ' for Ru^{II} complexes is close to unity[29]. In addition, as indicated by very low quantum yields of **2** and **Ru-P** (Table 2), k_o is much more significant in magnitude than the other terms in the denominator of this equation[30]. As a result, eq. 11 reduces to

$$-d[Ru^{2+}]/dt = (2.3\varepsilon\phi' I_o\tau_o l)\{(2k_e + k_x)[1] + k_d\}[Ru^{2+}] \quad (12)$$

with relationships $I_a = 2.3\varepsilon I_o[Ru^{2+}]l$ and $k_o = 1/\tau_o$, where ε and I_o are the extinction coefficient of Ru^{2+} and the intensity of the incident light, respectively, l is the thickness of the reaction vessel, and τ_o is the lifetime of the luminescence from $Ru^{2+}*$. Eq. 12 is combined with the experimentally determined rate equation, eq. 2, giving the relationship

$$k_{exp} = a(2k_e + k_x). \quad (13)$$
$$a = 2.3\varepsilon\phi' I_o\tau_o l$$

Taking into account $2k_e/k_x = Y/(X - Y)$, where X and Y are the percent conversion of **1** and the yield of **2** listed in Table 1, respectively, ak_e and ak_x for each reaction are evaluated from k_{exp} as summarized in Table 3. The rate constants evaluated yield a constant value of a, which is not determinable under the conditions of irradiation with multichromatic light.

On the other hand, $a = 1.5 \cdot 10^{-7}$ is obtained under irradiation with monochromatic light at 450 nm by taking into account $\varepsilon_{450} = 1.40 \cdot 10^4$ $cm^{-1}M^{-1}$, $I_o = 7.04 \cdot 10^{-6}$ einstein$\cdot s^{-1}$ under the conditions, and $l = 1$ cm, as well as by assuming $\tau_o = 650$ ns[30]. From this value of a, together with the rate constants ak_e and ak_x determined for the reactions with **1b** and **1d** under these conditions (entries 3 and 6 in Table 3), absolute rate constants k_e and k_x for these reactions are determined as shown in entries 2 and 4 in Table 5.

Then, using k_e and k_x for the reaction with **1b** as standards, absolute values of k_e and k_x for the other reactions are calculated (Table 5). The treatment is verified by the fact that the calculation reproduces the experimentally determined values of k_e and k_x for the reaction with **1d** (entry 4 in Table 5).

Energetics of the SET Process: The logarithms of k_e listed in Table 5 are plotted against peak potentials E_{ox}^{p} of **1** (Table 4) in Figure 4.

This results in an excellent linear correlation (correlation coefficient $r = 0.994$) covering various types of trivalent phosphorus compounds. The points for both aliphatic and aromatic trivalent phosphorus compounds fall on a single line, which is in sharp contrast to the findings for the SET quenching by amines. Photoreactions of chromium, iridium and ruthenium complexes[31] as well as of methylene blue[32] with amines have been investigated kinetically. The studies have shown that SET quenching of these photoexcited oxidants takes place more slowly with aliphatic amines than with aromatic amines, resulting in two distinct lines in the plots. It has been argued that the slower SET quenching by aliphatic amines results from the localization of the lone-pair n-electrons on the nitrogen atom, thus requiring greater reorganization energy during the SET. In the case of aromatic amines, on the other hand, π-π overlap between the aromatic rings of the amine quencher and of the oxidant

Scheme 2. Mechanism of the photoreaction of **1** with Ru^{2+} in methanol

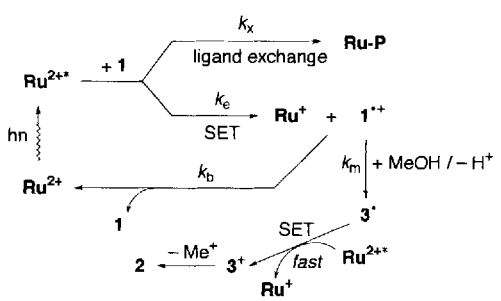

Table 5. Absolute rate constants for the SET and the ligand exchange

entry	1	$k_e \cdot 10^{-4}$ [a] [$M^{-1}s^{-1}$]	$k_x \cdot 10^{-5}$ [b] [$M^{-1}s^{-1}$]
1	**1a**	10.6	0.233
2	**1b**	(9.47)[c]	(1.91)[c]
3	**1c**	7.43	12.4
4	**1d**	7.16(6.73)[c]	4.28(4.33)[c]
5	**1e**	6.89	0.866
6	**1f**	4.67	8.21
7	**1g**	5.35	5.98
8	**1h**	3.72	8.31
9	**1i**	3.28	4.31
10	**1j**	3.61	3.7

[a] Calculated based on $k_e(\mathbf{1x}) = k_e(\mathbf{1b}) \times [ak_e(\mathbf{1x})/ak_e(\mathbf{1b})]$. – [b] Calculated based on $k_x(\mathbf{1x}) = k_x(\mathbf{1b}) \times [ak_x(\mathbf{1x})/ak_x(\mathbf{1b})]$. – [c] Values in parentheses denote the rate constants determined experimentally.

Figure 4. Plot of $\log k_e$ vs. E_p^{ox}. Filled and open circles denote the points for aromatic and aliphatic compounds, respectively

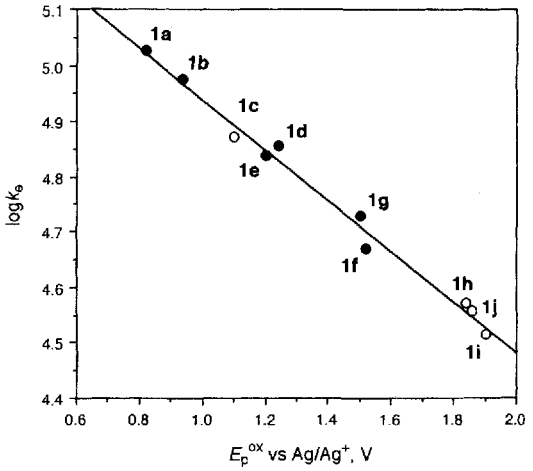

enhances the quenching rate. If such arguments hold true for the present reaction, the single line seen in Figure 4 is indication that for both the aliphatic and aromatic trivalent phosphorus compounds examined here, the *n*-electrons to be transferred are localized on the phosphorus atom, and that the aromatic ligands in aromatic trivalent phosphorus compounds are incapable of π-π overlap with bipyridine ligands in $\mathbf{Ru}^{2+}$*.

The slope of the plot ($\Delta \log k_e^{rel}/\Delta E_p^{ox}$) in Figure 4 provides additional important information. According to the Rehm-Weller theory[33], the slope is $-96500/2.3RT$ (= −17.2 at 20 °C) when the oxidation potential of the reductant is higher than the reduction potential of the oxidant. The slope for the present reaction should be of this magnitude since the measured peak oxidation potentials for the reductants, **1a–j**, are certainly higher than the reported value of the reduction potential for the oxidant, $\mathbf{Ru}^{2+}$* (E_{red}^0 = 0.84 V[12]). However, the experimentally determined slope of −0.46 is much less negative than expected from the theory. Weaker than expected dependences of SET quenching rates on oxidation potentials of quenchers have also been observed in the quenching of photoexcited states of transition metal complexes[31] and methylene blue[32] with aliphatic amines, whereas the SET quenching rate with aromatic amines depends on the oxidation potentials in accordance with the theory. The observations have been rationalized in terms of the formation of charge-transfer (CT) complexes between the photoexcited oxidants and aliphatic amines, within which SET takes place. Thus, our observation here (Figure 4) can be taken as an indication of CT complex formation between **1** and $\mathbf{Ru}^{2+}$*, with subsequent SET.

Photochemical Ligand Exchange of $\mathbf{Ru}^{2+}$ *with* **1**: Anticipating that bulkiness of **1** might regulate the rate of the ligand exchange, the logarithms of k_x listed in Table 5 were plotted against cone angles θ, this being a measure of the steric bulk of trivalent phosphorus compounds proposed by Tolman (Table 4)[34].

Figure 5. Scattered plot of $\log k_x$ vs. θ

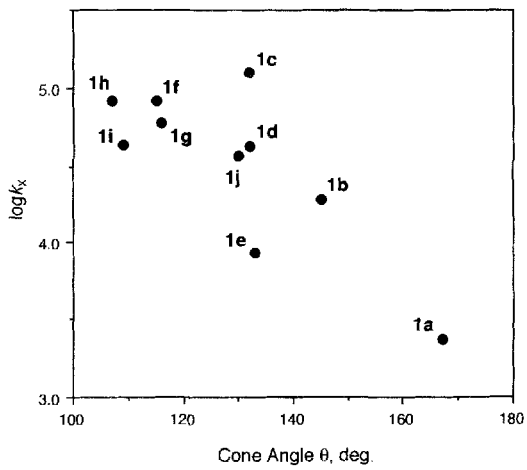

As can be seen in Figure 5, there is a tendency for **1** to become more reactive in ligand exchange as its cone angle decreases, but the correlation is rather poor (correlation coefficient, r = 0.79). Alternatively, an electronic factor in **1** may contribute to the rate of the ligand exchange. Such a factor of a trivalent phosphorus compound is represented by the CO stretching frequency ν of a transition metal carbonyl having the trivalent phosphorus compound as a ligand, e.g. $Ni(CO)_3(Z_3P)$[34][35]. It has been pointed out that ν is not affected by the bulkiness of the substituents on the phosphorus, so that it gives a convenient measure of a purely electronic factor. For a variety of trivalent phosphorus compounds, ν values are available[35], and if not, the values can be predicted by calculation[34]. Thus, $\log k_x$ was plotted against the values of ν listed in Table 4, but only a poor correlation resulted as shown in Figure 6.

Notable improvement in the correlation was obtained by linear combination of these parameters; an iterative calculation based on a dual-parameter equation proposed by Tolman (eq. 14)[34] eventually gave a best fit with α/β = 0.645 as shown in Figure 7 (correlation coefficient r = 0.89)[36].

$$\log k_x = \alpha\theta + \beta\nu \qquad (14)$$

The ratio of the coefficients α/β per se is not helpful for a quantitative evaluation of the relative importance of steric

Figure 6. Scattered plot of $\log k_x$ vs. ν

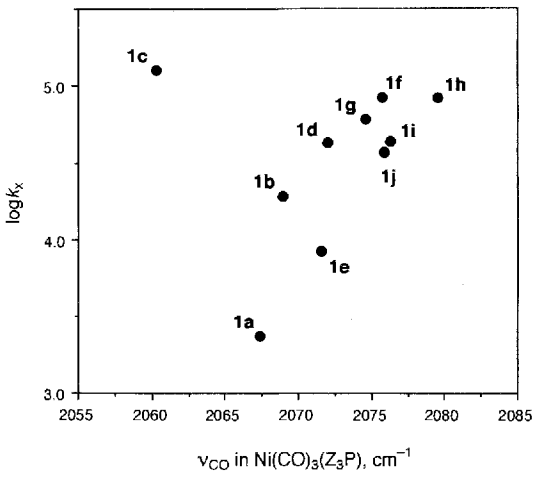

and electronic contributions to the rate of the ligand exchange; there are no pertinent data for comparison. It is nevertheless important to note that the rate of the ligand exchange is regulated by both steric and electronic factors in **1**.

Figure 7. Plot of $\log k_x$ vs. $\alpha\theta + \beta\nu$ ($\alpha/\beta = 0.645$)

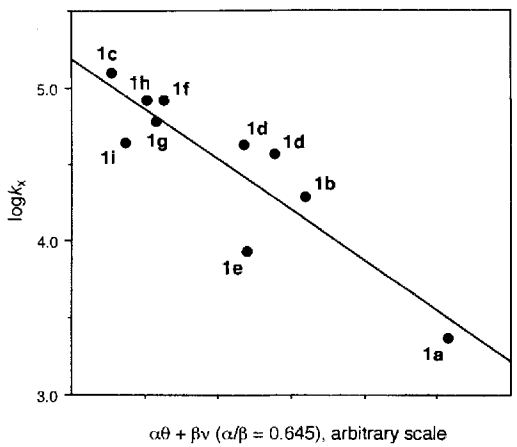

Several types of dual-parameter correlation analyses have been proposed to separate steric and electronic contributions in chemical reactions and physical properties[38][39]. For example, nucleophilic reactions of trivalent phosphorus compounds have been analyzed using a set of θ and pK_a [37] or a set of C_B and E_B values[40]. We also analyzed our data using these parameter sets. The correlation obtained in each analysis, although not fully satisfactory, showed significant improvement from correlations derived using a single parameter.

Competition Between SET and Ligand Exchange: At this point, a question arises about whether or not the one-electron donating ability and the nucleophilicity of **1** are related to each other. The answer seems to have already been presented in the above discussions. There are successes in individual interpretations of the energetics of SET and ligand exchange processes by using different parameters, respectively; the oxidation potentials of **1** are responsible for the rate of the SET from **1**, whereas the cone angles as well as the electronic factor represented by the ν values account well for the reactivity of the ligand exchange by **1**. Apparently, these parameters are not directly related to each other. In fact, tributylphosphane (**1c**) and phosphites (**1h–j**) have poor one-electron donor character but exhibit high nucleophilicity. The opposite is true for mesityldiphenylphosphane (**1a**) and triphenylphosphane (**1b**). We therefore tentatively conclude that the one-electron donor character and the nucleophilic character of trivalent phosphorus compounds are independent properties. However, further results are clearly required to verify this conclusion.

Nevertheless, the present study provides useful information for the development of organic syntheses in which trivalent phosphorus compounds are used as co-reagents. Conventional synthetic methods utilize the nucleophilic ability of trivalent phosphorus compounds[1], whereas new methods have recently been developed that depend on the electron-donating ability of these compounds[22][41]. In other words, choice of the trivalent phosphorus compound as a co-reagent is crucial to the success of trivalent phosphorus-mediated organic syntheses. Our findings provide useful data relevant to this matter.

This work was supported in part by a Grant-in-Aid for Scientific Research (C) (No. 09640654) from the *Ministry of Education, Science, Sports, and Culture, Japan*. One of the authors (S.Y.) acknowledges the financial support of a *Tezukayama Research Grant* in 1996.

Experimental Section

Instruments: UV/visible spectra were recorded on a Shimadzu UV-2200A recording spectrophotometer. Luminescence from $\mathbf{Ru}^{2+}$* was monitored on a Shimadzu RF-5000 spectrofluorophotometer. – GC analysis was performed on a Shimadzu GC 14A gas chromatograph. – Mass spectra were obtained on a Shimadzu GCMS-QP2000A gas chromatograph-mass spectrometer equipped with a Shimadzu GC-MSPAC 200S data processor. – ^{1}H- and ^{31}P-NMR spectra were obtained on a Varian XL 200 NMR spectrometer operating at 200 MHz and 81 MHz, respectively. – Oxidation peak potentials of **1** were measured on a Cypress Systems OMNI 90 potentiostat in acetonitrile using a platinum working electrode, an Ag/Ag^+ reference electrode, and tetraethylammonium tetrafluoroborate (0.10 M) as the supporting electrolyte.

Materials: Mesityldiphenylphosphane (**1a**) was prepared by a conventional Grignard method based on a literature procedure[42]. Triphenylphosphane (**1b**) (Nacalai Tesque) and tributylphosphane (**1c**) (Kanto Chemical) were obtained from commercial sources. Phosphites **1h–j** were also commercially available (Tokyo Chemical Industry) and were distilled before use. Preparation methods for phosphinites **1d–e**[43] and phosphonites **1f–g**[44] have been described previously. Tris(2,2′-bipyridyl)ruthenium(II) chloride hexahydrate, $Ru(bpy)_3Cl_2 \cdot 6\ H_2O$ ($\mathbf{Ru}^{2+}$), was prepared from ruthenium(II) dichloride according to a literature procedure[44] and was purified by recrystallization from water.

General Procedures: A solution of $\mathbf{Ru}^{2+}$ in methanol ($2.50 \cdot 10^{-5}$ M) was irradiated with light from an Ushio xenon arc short lamp

UXL-500D-0 through a Toshiba sharp-cut filter L-39 (irradiation at $\lambda > 360$ nm) or a Toshiba interference filter KL-45 (irradiation at $\lambda = 450$ nm) in the presence of a 10-fold excess of **1** under an argon atmosphere at 20 °C. The UV/visible spectrum of the reaction mixture was recorded at intervals. Photolysis was also carried out with concentrations of **1** and $\mathbf{Ru}^{2+}$ of $5.00 \cdot 10^{-3}$ M under the conditions described above. After ca. 5–7 hours, the reaction mixture was passed through a short silica gel column to remove non-volatile materials, and the filtrate was analyzed by GC. The products were identified by comparison of their retention times with those of authentic samples. The yields of the products were determined by GC using dodecane, octadecane or eicosane as an internal standard. Analysis by GC-MS or NMR spectroscopy was performed if necessary. To isolate non-volatile products, the solution of **1** and $\mathbf{Ru}^{2+}$ in methanol ($5.00 \cdot 10^{-3}$ M) was photolyzed for 6 hours. The resulting reaction mixture was concentrated in vacuo, and dichloromethane was added to the residue. Insoluble material (mostly the starting ruthenium complex $\mathbf{Ru}^{2+}$) was filtered off, and the filtrate was again concentrated in vacuo. The residue was purified by repeated recrystallization from dichloromethane to give reddish-brown crystals. By comparison of the UV/visible and ^{31}P-NMR spectra with those of authentic samples of **Ru-P** and **Ru-Cl**, which were prepared independently according to the conventional method, this material was found to be a ruthenium complex **Ru-P** contaminated with a trace of a complex **Ru-Cl**. The yield of **Ru-P** was determined based on the absorbance at 465 nm in the UV/visible spectrum of this material. Due to the contamination with **Ru-Cl**, elemental analysis of **Ru-P** was not reliable.

Actinometry: A vessel containing a solution of potassium trioxalatoferrate(III) ($6.00 \cdot 10^{-3}$ M) in 0.05 M aqueous sulfuric acid was put in the place of the reaction vessel and irradiated with the light from a xenon lamp through a Toshiba KL-45 interference filter. By measuring the amount of the photoreduction product, the Fe^{II} complex, the intensity of the incident light on the reaction vessel was determined[45]. In calculating the quantum yields of the products, it was taken into account that the area of the vessel irradiated was 4 cm^2.

Kinetics: A quartz cell (1-cm thick) containing a solution of $\mathbf{Ru}^{2+}$ ($1.0 \cdot 10^{-5}$ M) and **1** [$(1.0-3.0) \cdot 10^{-4}$ M] in methanol was irradiated with a light from a xenon lamp through an appropriate glass filter. The temperature of the solution was maintained at 20 °C by circulating thermostatted air throughout the course of the irradiation.

[1] B. P. Mundy, M. G. Ellerd, *Name Reactions and Reagents in Organic Synthesis*, Wiley, New York, **1988**.
[2] S. Yasui, *Rev. Heteroatom Chem.* **1995**, *12*, 145–161 and references cited therein.
[3] [3a] S. Yasui, A. Ohno, *Tetrahedron Lett.* **1991**, *32*, 1047–1050. – [3b] S. Yasui, K. Shioji, M. Yoshihara, T. Maeshima, A. Ohno, *Tetrahedron Lett.* **1992**, *33*, 7189–7192. – [3c] S. Yasui, K. Shioji, A. Ohno, M. Yoshihara, *Chem. Lett.* **1993**, 1393–1396. – [3d] S. Yasui, K. Shioji, A. Ohno, *Heteroatom Chem.* **1994**, *5*, 85–90. – [3e] S. Yasui, K. Shioji, A. Ohno, M. Yoshihara, *J. Org. Chem.* **1995**, *60*, 2099–2105.
[4] [4a] S. Yasui, M. Fujii, C. Kawano, Y. Nishimura, A. Ohno, *Tetrahedron Lett.* **1991**, *32*, 5601–5604. – [4b] S. Yasui, M. Fujii, C. Kawano, Y. Nishimura, K. Shioji, A. Ohno, *J. Chem. Soc., Perkin. Trans. 2* **1994**, 177–183. – [4c] S. Yasui, K. Shioji, A. Ohno, *Tetrahedron Lett.* **1994**, *35*, 2695–2698. – [4d] S. Yasui, K. Shioji, A. Ohno, *Heteroatom Chem.* **1995**, *6*, 223–233.
[5] S. Yasui, K. Shioji, M. Tsujimoto, A. Ohno, *Chem. Lett.* **1995**, 783–784.
[6] R. L. Powell, C. D. Hall, *J. Am. Chem. Soc.* **1969**, *91*, 5403–5404.
[7] M. Ochiai, M. Kunishima, Y. Nagao, K. Fuji, E. Fujita, *J. Chem. Soc., Chem. Commun.* **1987**, 1708–1709.
[8] G. Pandey, D. Pooranchand, U. T. Bhalerao, *Tetrahedron* **1991**, *47*, 1745–1752.
[9] S. Takagi, T. Okamoto, T. Shiragami, H. Inoue, *J. Org. Chem.* **1994**, 7373–7378.
[10] C. Creutz, N. Sutin, *Inorg. Chem.* **1976**, *15*, 496–499.
[11] S. Fukuzumi, S. Koumitsu, K. Hironaka, T. Tanaka, *J. Am. Chem. Soc.* **1987**, *109*, 305–316.
[12] C. Creutz, N. Sutin, *J. Am. Chem. Soc.* **1976**, *98*, 6384–6385.
[13] C. P. Anderson, D. J. Salmon, T. J. Meyer, R. C. Young, *J. Am. Chem. Soc.* **1977**, *99*, 1980–1982.
[14] T. E. Mallouk, J. S. Krueger, J. E. Mayer, C. M. G. Dymond, *Inorg. Chem.* **1989**, *28*, 3507–3510.
[15] B. Durham, J. V. Caspar, J. K. Nagle, T. J. Meyer, *J. Am. Chem. Soc.* **1982**, *104*, 4803–4810.
[16] N. Nagao, M. Mukaida, E. Miki, K. Mizumachi, T. Ishimori, *Bull. Chem. Soc. Jpn.* **1994**, *67*, 2447–2453.
[17] B. Durham, J. L. Walsh, C. L. Carter, T. Meyer, *J. Inorg. Chem.* **1980**, *19*, 860–865.
[18] J. E. Figard, J. D. Petersen, *Inorg. Chem.* **1978**, *17*, 1059–1063.
[19] J. Van Houten, R. J. Watts, *Inorg. Chem.* **1978**, *17*, 3381–3385.
[20] Kinetic measurements were also made by following the decrease in the absorption from $\mathbf{Ru}^{2+}$. This led to almost identical results but with much poorer reliability due to increasing absorbances from the products $\mathbf{Ru}^{+}$ and **Ru-P**.
[21] Due to the lower intensity of the monochromatic light at 450 nm, photolysis with this light gave smaller values of k^{obs} (of the order of 10^{-5} s^{-1}) and k_d^{obs} ($8.97 \cdot 10^{-6}$s^{-1}), which are close to the lower limit of precise determination. For this reason, we performed most of our experiments using the light of $\lambda > 360$ nm.
[22] S. Ganapathy, K. P. Dockery, A. E. Sopchik, W. G. Bentrude, *J. Am. Chem. Soc.* **1993**, *115*, 8863–8864.
[23] Half-wave potentials of $Ph_nR_{(4-n)}P^+$ ($n = 1$–4, R = alkyl) have been reported as being −1.6 – (−2.2 V) vs. Ag/Ag$^+$. L. Horner, F. Röttger, H. Fuchs, *Chem. Ber.* **1963**, *96*, 3141–3147.
[24] K. P. Dockery, W. G. Bentrude, *J. Am. Chem. Soc.* **1994**, *116*, 10332–10333.
[25] The ionization energy of methanol is about 11 eV[26a], which is 1.5 eV higher than that of **1h**[26b].
[26] [26a] N. L. Ma, B. J. Smith, J. A. Pople, L. Radom, *J. Am. Chem. Soc.* **1991**, *113*, 7903–7912. – [26b] L. Zeller, J. Farrell, Jr., P. Vainiotalo, H. I. Kenttämaa, *J. Am. Chem. Soc.* **1992**, *114*, 1205–1214.
[27] It has been shown that spin-orbit coupling in the MLCT photoexcited state of $\mathbf{Ru}^{2+}$, $\mathbf{Ru}^{2+*}$, is so great as to make spin labelling for this state meaningless. Accordingly, use of the term "intersystem crossing" is not appropriate here. [27a] R. W. Harrigan, G. A. Crosby, *J. Chem. Phys.* **1973**, *59*, 3468–3476. – [27b] G. D. Hager, G. A. Crosby, *J. Am. Chem. Soc.* **1975**, *97*, 7031–7037. – [27c] G. D. Hager, R. J. Watts, G. A. Crosby, *J. Am. Chem. Soc.* **1975**, *97*, 7037–7042. – [27d] K. W. Hipps, G. A. Crosby, *J. Am. Chem. Soc.* **1975**, *97*, 7042–7048.
[28] Ionic reactions of $Z_3P^{\bullet+}$ with alcohols are largely regulated by the steric bulk of the alcohol. Since methanol is very small, the rate is essentially independent of $Z_3P^{\bullet+}$. See ref.[5]
[29] J. N. Demas, D. G. Taylor, *Inorg. Chem.* **1979**, *18*, 3177–3179.
[30] [30a] J. Fan, S. Tysoe, T. C. Strekas, H. D. Gafney, N. Serpone, D. Lawless, *J. Am. Chem. Soc.* **1994**, *116*, 5343–5351. – [30b] E. Sabatani, H. D. Nikol, H. B. Gray, F. C. Anson, *J. Am. Chem. Soc.* **1996**, *118*, 1158–1163.
[31] R. Ballardini, G. Varani, M. T. Indelli, F. Scandola, V. Balzani, *J. Am. Chem. Soc.* **1978**, *100*, 7219–7223.
[32] R. H. Kayser, R. H. Young, *Photochem. Photobiol.* **1976**, *24*, 395–401.
[33] D. Rehm, A. Weller, *Israel J. Chem.* **1970**, *8*, 259–271.
[34] [34a] C. A. Tolman, *J. Am. Chem. Soc.* **1970**, *92*, 2953–2956. – [34b] C. A. Tolman, *Chem. Rev.* **1977**, *77*, 313–348.
[35] W. Strohmeier, F.-J. Müller, *Chem. Ber.* **1967**, *100*, 2812–2821.
[36] As has been pointed out in a similar correlation analysis, the coefficients α and β must bear different units to accommodate each term in eq. 14 in the energy term. It has been shown, for example, that the term including θ should be connected with an energy term such as $\Delta G^{\ddagger} \approx f\theta$, where f is the molecular force constant. See ref.[37]
[37] P. M. Zizelman, C. Amatore, J. K. Kochi, *J. Am. Chem. Soc.* **1984**, *106*, 3771–3784.
[38] R. W. Taft, Jr., *J. Am. Chem. Soc.* **1952**, *74*, 3120–3128.

[39] J.-I. Isizawa, K. Sakakibara, M. Hirota, *Bull. Chem. Soc. Jpn.* **1996**, *69*, 1003–1015.
[40] R. S. Drago, S. Joerg, *J. Am. Chem. Soc.* **1996**, *118*, 2654–2663.
[41] H. K. Nair, D. J. Burton, *J. Am. Chem. Soc.* **1994**, *116*, 6041–6042.
[42] M. Culcasi, Y. Berchadsky, G. Gronchi, P. Tordo, *J. Org. Chem.* **1991**, *56*, 3537–3542.
[43] S. Yasui, K. Shioji, M. Yoshihara, T. Maeshima, A. Ohno, *Bull. Chem. Soc. Jpn.* **1993**, *66*, 2077–2083.
[44] R. A. Palmer, T. S. Piper, *Inorg. Chem.* **1966**, *5*, 864–878.
[45] C. G. Hatchard, C. A. Parker, *Proc. Roy. Soc.* **1956**, *A 235*, 518–536.

[97091]